Biogeosciences Discuss., 7, 4385–4424, 2010
www.biogeosciences-discuss.net/7/4385/2010/
doi:10.5194/bgd-7-4385-2010

Biogeosciences Discussions

Modelling burned area in Africa

V. Lehsten[1], P. Harmand[2], I. Palumbo[3,*], and A. Arneth[1]

[1]Division of Physical Geography and Ecosystems Analysis (ENES), Department of Earth and Ecosystem Sciences, Lund University, Sweden
[2]Institut für Mathematik, Universität Oldenburg, Germany
[3]Department of Geography, University of Leicester, University Road, Leicester LE17RH, UK
[*]currently at: DG Joint Research Centre – European Commission, Ispra, Italy

Received: 18 February 2010 – Accepted: 30 May 2010 – Published: 10 June 2010

Correspondence to: V. Lehsten (veiko.lehsten@nateko.lu.se)

Published by Copernicus Publications on behalf of the European Geosciences Union.

Abstract

The simulation of current and projected wildfires is crucial for predicting vegetation as well as pyrogenic emissions in the African continent. This study uses a data-driven approach to parameterize burned area models applicable to dynamic vegetation models (DVMs) and global circulation models (GCMs). Therefore we restricted our analysis to variables for which either projections based on climate scenarios are available, or which are calculated by DVMs and the spatial scale to one degree spatial resolution, a common scale for DVMs as well as GCMs.

We used 9 years of data (2000–2008) for the variables tree and herb cover, precipitation over the last dry season, wet season and averaged over the last 2 years, a fire-danger index (the Nesterov index), population density and an annual proportion of area burned derived from the MODIS MCD45A1 product. Since the effect of fires on vegetation depends strongly on burning conditions, the timing of wildfires is of high interest too. We related the seasonal occurrence of wildfires to the Nesterov index and found a lognormal relationship with a maximum at a value of 10^4.

We parameterized two generalized linear models, one with the full variable set (model I) and one (model II) considering only climate variables. All introduced variables resulted in an increase in model performance. Model I correctly predicts the spatial distribution and extent of fire prone areas though the total variability is underrepresented. Model II has a much lower performance in both aspects (correlation coefficient of predicted and observed ratio of burned area: 0.71 model I and 0.58 model II). An application of the models with simulated climate data ranging from 1980 to 2060 resulted in a strong decrease of burned area of ca. 20–25%. Since wildfires are an integral part of land use practices in Africa, this indicates a high loss in areas favourable for food production.

BGD

7, 4385–4424, 2010

1 Introduction

Wildfires are a global phenomenon with direct effects on vegetation, the local and global atmospheric chemistry, as well as for the population inhabiting the affected areas. The African continent has the highest amount of annual burned area globally (Roy et al., 2008) with extensive wildfires activities in African savannas tracing back through the Quaternary period (Bird and Cali, 1998). Over the (mostly low industrialized) African continent, the amount of pyrogenically released carbon is estimated to be in the same order of magnitude as the carbon released by fossil fuel burning (Williams et al., 2007). Not only the pyrogenic carbon release is of interest (e.g. for global circulation models; GCMs) but also fire-feedback on vegetation structure. Dynamic vegetation models (DVMs; Arneth et al., 2010b) such as LPJ-GUESS (Smith et al., 2001) or CASA (Potter et al., 1993) simulate vegetation and its atmospheric exchange depending on historic and projected climate data, and in fire-prone environments their results rely strongly on the fire model used (Arneth et al., 2010b).

Some DVM studies investigating the effects of wildfires have used either remotely sensed burned area data (van der Werf et al., 2006; Lehsten et al., 2009) or a dynamic mechanistic burned area model derived from theoretical considerations (Thonicke et al., 2010; Arneth et al., 2010a). The former can only be applied for the period when remote sensing products are available; the latter is appropriate to analyse past and future changes in fire regimes. While some variables relevant for wildfires which are very scale dependent (e.g. slope) might be neglected at larger scale, the assumption of a mean value over a typical gridcell of the available meteorological data is more problematic for other variables. This is especially the case for wind speed which is very important for the fire development, spread and intensity and varies strongly at a local scale. It is even influenced by the fire itself due to uplift, given a sufficiently large fire. Mechanistic burned area models derived from applications of fire spread models thereby suffer from highly uncertain parameterisations of some processes that are relevant for burnt-area calculation (like horizontal wind speed, fire travel in fragmented

BGD
7, 4385–4424, 2010

landscape, etc.) and require some statistical assumptions for parts of the calculation e.g. the relationship between population density and potential ignitions in the latter case. These uncertainties are amplified by subsequent simulations of fire spread.

Our study seeks to parameterise a statistical model for the prediction of burned area based on its major controlling factors. We use remotely sensed data of burned area combined with climate and population density data to optimise a statistical model for the prediction of wildfire activity. Despite its importance for climate change assessments, atmospheric composition and ecology, the analysis of the factors controlling wildfires is in a relatively early stage especially at a continental scale. This is partly due to the lack of multi-annual high resolution remote sensing data of burned areas in the past (Roy et al., 2010). Though such models are of high interest in themselves, they are only applicable to DVMs or GCMs if they are restricted to climate and socio-economic variables, which have a historic and projected global coverage, at a spatial scale typical of DVMs (i.e. between 0.25° and 1° latitude) and use a fire model structure that is suitable to be incorporated in dynamic models.

Here we analyze the relationship between annual burned ratio, climatic drivers, vegetation and population density. The resulting fire model is readily applicable to estimate burned area and can be incorporated in dynamic vegetation models or global circulation models.

After demonstrating the performance of the model with recent climate data we also apply it to climate change projections of the SRES A2 and B1 scenarios. While GCMs deliver projections of climate variables, they do not provide the estimates for tree cover and herb cover which have been shown to be important determinants of wildfires in previous studies (e.g. Archibald et al., 2008), which are commonly estimated within a DVM and can potentially interact strongly with the simulated fire pattern. We simulate total burned area of Africa from 1980 to 2060 using burned area models, one containing climate and vegetation related variables and a second one with a reduced variable set containing only climate related variables.

BGD
7, 4385–4424, 2010

2 Methods

2.1 Data selection

We considered the period from 2000 to 2008 over the full availability of the MODIS MCD45 burned area product (Roy et al., 2008), resulting in eight "fire years" (see below). The burned area data were separated into three sets: a training dataset, a validation dataset and a dataset only used to evaluate the spatial patterns of the prediction. The training dataset contained all data except for a longitudinal band from 20°–30° (Fig. 1) and all data from the year 2007 and was used to estimate the model parameters. The validation dataset contained the longitudinal band from 20°–30° (Fig. 1) for all years and was used to calculate the correlation coefficients (R-values; see below). When testing the relationship between spatial distributed variables it is common practice to separate the dataset randomly between training data and validation data, and to repeat the procedure of generating training and evaluation data to generate a large number of models. This allows evaluating the variation of performance among the estimated models. However, we decided to use a single, spatially and temporally predefined validation dataset because a bootstrapping procedure of randomly assigning data points to either the training or validation dataset results in different model parameter for each model. Since our focus lies on the estimation of these parameters for further application we aimed for a single model and choose the validation data in a way that it covers as much variation as possible with respect to the variables by using a cross continental longitudinal band. By assigning data from all years to the validation data, instead of using e.g. a single year as validation we assured that no spatial location that contributed to the training data is used in the validation dataset. The third dataset, containing only the year 2007 was used to evaluate the spatial performance of the model and to display the spatial patterns of the differences between model predictions and data at continental scale.

BGD
7, 4385–4424, 2010

2.1.1 Burned area

Since the fire seasons are different in the Northern and Southern Hemisphere, burned fractions for both hemispheres were calculated for different time periods. The "fire year" was set to last from the 1st April until the 31st March in the Northern Hemisphere, whereas in the Southern Hemisphere it spans from 1st November–31st October (for details see Lehsten et al., 2010). While fire seasons are defined as times with considerable amounts of burned area (see Results section), we separated the data into "fire years" spanning a whole year, including the fire season (called dry season in the remaining parts) as well as the preceding wet season, see below. This allowed us to pool Northern and Southern Hemisphere Africa into a single dataset.

We used the burned area data MODIS MCD45 (Roy et al., 2008). The maps come as monthly data with 500 m resolution and were combined to obtain annual datasets for the period 2000–2008. The MCD45 product is known to underestimate the total burned area (Roy, 2009) therefore we used the lowest quality stage of the burned area data, which has the highest level of detection of burned area (and also the highest level of incorrectly detected burned areas). All pixels classified as 1'unsuitable" in the MODIS product were discarded. Since we used a one degree grid for the analysis, information on the fire occurrence based on 500 m pixels has been transformed to a burn ratio over each one degree cell. The annual burned area (Fig. 1 and 3a) was derived from the monthly maps without specifically accounting whether a pixel was classified as "burned" once or more times in the same "fire year". We calculated an annual "burn ratio" value for each grid cell from the 500 m pixels of the MCD45 product by calculating the ratio between the number of pixels classified as 'burned' over the 12-month period and the total number of valid pixels within the same grid cell. We thereby assumed indirectly that the pixels that were not classified in the MODIS product experience the same fire frequency as the classified pixel.

We consider the use of burned area data more reliable than active fire data converted into burned area data based on the fractional tree cover (e.g. Pechony and Shindell,

BGD
7, 4385–4424, 2010

2009) since the time period of potential detection for burned area is higher than that of active fires. Active fire data only takes into account fires occurring during the satellite overpass in cloud-free conditions. Therefore polar-orbiting satellites can only provide partial information on the fire activity. In Africa this is particularly relevant since fires usually last only few hours or less (though some large fires might last for several days in the absence of fire breaks) and as a consequence the non-detection rate of fires in hot spot products is relatively large. Moreover the conversion of fire counts into burned areas introduces a high uncertainty since the conversion factor from one detected active fire 500m pixel to the burned area ranges from about 0.2 to 6 (Giglio et al., 2006). A recent validation exercise of the burned area products: L3JRC (Tansey et al., 2008), GlobCarbon (Simon et al., 2004) and MODIS MCD45 (Roy et al., 2008) against classified 5 km×5 km Landsat scenes of southern Africa found highest level of agreement for the MODIS product, resulting in a correlation coefficient $R = 0.86$ ($R^2 = 0.75$) and a slope of 0.75.

2.1.2 Tree and herb cover

Fuel estimation in savannah regions from remotely sensed data is not well established. Mbow et al. (2004) used spectral parameter for wetness, brightness and greenness as a proxy, which can be derived from satellite data but might not be straight forward to be calculated within DVMs. We therefore used fractional cover of trees and herbs since these variables can be assessed from remotely sensed data and are very likely to be calculated within most DVMs. Trees provide in combination with the grassy vegetation the fuel (mainly litter) required for a wildfire to burn. Their relative cover is expected to influence wildfires in a number of ways. In African savannas tree cover can be associated with fuel production and burning conditions. Low tree cover indicates dry conditions with low fuel production and infrequent fires since the fuel needs to accumulate over several years, while a high tree cover can be linked to moist and therefore unfavourable burning conditions. Savannahs as well as natural and semi-natural grasslands in the wet-dry tropics are particularly fire prone due to the use of

BGD
7, 4385–4424, 2010

fire as a common landscape management tool to enhance grass re-growth for grazers and to avoid shrub encroachment (Saarnak, 2001; Mbow, 2000; Hough, 1993). Archibald et al. (2008) in their investigation of drivers of burned area found tree cover to have the highest predictive value.

Woody and herbaceous vegetation data were generated by up-scaling the MODIS Vegetation Continuous Fields product (VCF; Hansen et al., 2003). This product provides information of the tree, herbaceous vegetation and bare ground fractions at 500 m resolution for the year 2001. Since the three fractions sum up to a maximum of 100%, no information is available on possibly overlapping layers of vegetation (like forests understorey). The savannah ecosystems in Africa can show vegetation strata with grass and shrubs mixed in the same patch. However, most savannah areas, which are burning frequently, have no closed canopies like rainforests, making the detection of understorey grasses possible for the satellite. Though tree and herb cover are expected to change over the course of time, to our knowledge there is not continuous product available for the investigated time period. Given that the data are aggregated to one degree spatial resolution, we expect however only a low year to year variability at this scale at least over the time period of our analysis. However, over the time period used to project the burned area, this ratio might change considerably

2.1.3 Population density

Since the vast majority of burned area is ignited by humans (Saarnak, 2001), population density is expected to have an effect on it. Venevsky et al. (2002) used an exponential function to relate the number of ignitions by humans to population density. This steadily increasing relationship is subsequently multiplied with a spatially explicit calculated factor of human ignition potential (ignitions per person per day; derived from remote sensing data) which includes effects of urbanity and typical land use practices. This approach has been further developed by Thonicke et al. (2010) in applying a uni-modal shaped relationship between population density and number of potential ignitions reflecting the fact that a certain minimum population density is required in order

BGD
7, 4385–4424, 2010

to maintain land use systems which can make use of fire as a landscape management tool. At higher population densities urbanisation limits the application of fires as well as it increases the efforts to prevent fires.

For our analysis we used the dataset for population density (raster dataset; resolution 5*5 arc minutes) provided from the FAO available for the years 2000 and 2005 and as projection for 2010 (Healy, 2008). We scaled the data to 1 degree latitude and longitude and interpolated intermediate years linearly.

For the application of the parameterised model we used the gridded population projection from Bengtsson et al. (2006) for the two SRES storylines B1 and A2 (Fig. 2).

2.1.4 Precipitation

Precipitation is the main driver of net primary production and thereby of fuel load. Several aspects of precipitation are potentially influencing wildfires: Spessa et al. (2005) as well as Lehsten et al. (2009) found a uni-modal relationship between total precipitation sum and the amount of burned area. Harris et al. (2008) found a strong relationship between the burned area and the precipitation of the preceding wet season in northern Australia. As suggested by Van Wilgen (2004) we also tested the influence of the mean precipitation of the last two dry and wet seasons since there seems to be a certain time required to build up fuel loads in order to maintain a wildfire.

We used the TRMM data (Kummerow et al., 1998). From this originally daily precipitation data we generated three precipitation sums, reflecting our fire year definition. One for the potential dry season (NHA: Oct–Mar, SHA: May–Oct), capturing burn conditions over the dry period, one for the potential wet season (NHA: Apr–Sep; SHA Nov–Apr), as the period that determines the potential fuel load of the given year, and one for the average precipitation over the last two wet and dry seasons, representing the potential fuel accumulation.

BGD
7, 4385–4424, 2010

2.1.5 Nesterov index

An obligatory condition for wildfire development is amongst fuel and ignition sources also a sufficient dryness of the fuel. Fuel dryness is related to the Nesterov fire-hazard-index (short Nesterov index; Nesterov, 1949; Thonicke et al., 2010).

This index ($Nest_d$) depends on daily precipitation (p_d) and the mean and dewpoint temperatures (t_{mean} and t_{dew}). For days with precipitation below 3 mm the index is computed as in (1) and it is (re)set to zero if the daily precipitation is above 3 mm (2). The Nesterov index has been originally developed for boreal areas and hence is also reset to zero if the temperature drops below zero degrees Celsius. Since there are regions in Africa where neither low temperature nor daily precipitation above 3 mm occur over several years, we limited this statistic to a maximum value of 200 000 to avoid unreasonably high values being reached (3).

$$Nest_d = (t_{mean} - t_{dew}) t_{mean} + Nest_{d-1} \text{ if } p_d < 3\text{mm} \quad (1)$$

$$Nest_d = 0 \text{ if } p_d \geq 3\text{mm} \quad (2)$$

$$Nest_d = 200\,000 \text{ if } Nest_d \geq 200\,000 \quad (3)$$

Since the dewpoint temperature was not available in the datasets, we approximated it as follows:

$$t_{dew} = \frac{237.7°\text{C}\left(\frac{17.271 * t_{mean}}{237.7°\text{C} + t_{mean}} + \ln(h_r)\right)}{17.271 - \frac{17.271 * t_{mean}}{237.7°\text{C} + t_{mean}} + \ln(h_r)} \quad (4)$$

with t_{mean} and t_{dew} being the mean and dewpoint temperatures and h_r being the relative humidity ranging from 0 to 1 (Foken, 2003 p. 43) .

The Nesterov index varies daily. In the first part of our statistical analysis we used the maximum value over each grid cell for each "fire year", while for estimation of the seasonal occurrence of wildfires we used the daily values. Here we used a Hovemöller

BGD
7, 4385–4424, 2010

plot to display the average Nesterov index over the course the year per longitudinal band of one degree width. For all cells which experienced a higher burned area ratio than 0.1 percent, we also related the sum of burned area ratios to the corresponding Nesterov index.

2.2 Data analysis

All data were re-gridded to 1 degree resolution. Logistic regression models with quadratic terms (generalized linear models; GLMs; Eq. 5) have been generated pooling all 8 "fire years" of data. These models evaluate the probability of a certain event (the area being burned) in relation to a certain variable (e.g. ratio of tree cover), or combinations of variables. In cases where the relationship between burned area and the investigated variable was asymmetrical (skewed) we used the logarithm of the variable as input (e.g. burned area vs. population density; Fig. 3f). For each one degree cell the amount of data used to estimate the parameter is equal to the number of successfully classified 500 m MCD45 pixels. For each parameterisation we calculated a correlation coefficient (R-value) by correlating the observed burned areas to the predicted values derived from the model estimation for the evaluation dataset.

Two models were parameterised: model I derived from the full set of variables and model II derived only from the climate variables not containing tree and herb cover.

2.2.1 Model choice: Baysian Information Criterion (BIC)

All incorporated variables are to a certain degree correlated with each other. The sum of tree cover and herb cover can result in a maximum of 100%. All the precipitation variables can be expected to exert a certain degree of dependence, spatially as well as temporally. Due to the low rate of industrialization, the population density can be expected to depend on the ability of the surrounding area to produce food, which again is directly related to the annual rainfall. Since all variables quantify different aspects of the grid cell which potentially influence the burned area we decided to base the decision

BGD
7, 4385–4424, 2010

to include or discard them not on their level of correlation but on the improvement of the final model.

To evaluate whether the incorporation of additional parameter in the model increased the quality of the model or simply increased the correlation factor due to over-fitting we used the Bayesian Information Criterion. This criterion is known to penalize additional parameters stronger than the Akaike criterion (Schwarz, 1978). The model with smallest BIC is considered the best. To test whether the BIC values differ significantly, we used a bootstrapping procedure which consists of resampling the dataset 10^3 times and subsequent parameter estimation. BIC values for each variable combination were then compared with the variable combination containing one variable more using the Wilcoxon signed rank test at the 5% significance level. Variables were considered to significantly improve the model performance if the BIC values decreased significantly.

2.3 Model application – climate scenarios

To show to applicability of the parameterised model, and to assess the expected trend of burned area in the African continent, we applied it to simulated climate data for the two SRES storylines A2 and B1. We used the 6 hourly values provided from the World Data Center for Climate i.e. the experiments EH5-T63L31_OM_20C3M_1_6H, EH5-T63L31_OM-GR1.5L40_A2_1_6H and EH5-T63L31_OM-GR1.5L40_B1_1_6H (Roeckner, 2005) to calculate the required variables (see Fig. 2). We combined the first dataset containing simulated climate data for the 20th century to each of the other two which contained the projected climate to obtain two time series spanning from 1980 till 2060 and calculated the resulting total burned area. Since there are no projections of tree and herb cover available for the 21^{th} Century, we parameterised two sub-models one (model I) with and one without (model II) tree and herb cover. For the projection of burned area using model I we assumed the tree and herb cover to be fixed over the simulation period.

BGD
7, 4385–4424, 2010

3 Results

The relationship between each variable and the fraction of burned area is displayed in Fig. 3. All variables show a uni-modal response, though for some of them logarithms were taken in order to make the response more symmetric. The p-values of all GLMs, testing the difference to zero for all model parameter of the modelled response (red lines) are below 10^{-4}, indicating a uni-modal distribution rather than a linear distribution of the data.

To assess the explanatory value of each descriptive variable we listed the correlation coefficients (R-values) of the single variables (Table 1) using the parameters estimated from the training data and assessing the correlation between the predicted and the remotely sensed burned area from the validation dataset. After estimating the fit of models using only one variable, we generated cumulative models adding one variable after the other and calculated BIC values. A test of difference revealed that each variable increased the performance of the cumulative model. The final model containing all variables (model I) resulted in an R-value of 0.71 and if only climate related variables are considered (model II) a lower R-value of 0.58. Correlating the predicted values of the training datasets with the observed values of the training dataset using model I results in an R-value of 0.74 (model II: 0.60).

For the variables dry season precipitation and population density we used the natural logarithm instead of the actual value.

$$ba = \frac{1}{1 + e^{-\left(a + \sum_{i=1}^{7} l_i v_i + s_i v_i^2\right)}} \quad (5)$$

The model has one parameter for the linear part l_1 to l_7 for each variable v_1 to v_7 and another one (s_i) for the squared part. All parameter of model I are listed in Table 1. The final model I also has a constant term (a) of −10.6 (Eq. 5; Table 1). The parameter and R-values of model II are listed in Table A1 in the Appendix.

BGD
7, 4385–4424, 2010

The predicted and observed burned area as well as the residuals for the "fire year" 2007 are shown in Fig. 4 for model I and Fig. A1 in the Appendix for model II.

Model I performs well in predicting absence of notable burned area in very dry areas like the Sahara or Kalahari desert and in wet areas like the tropical rain forest. It captures the geographic distribution of fires across the savannah biome well, but does not pick up high burned area fractions above 0.5. Overall the predicted burned area shows a lower spatial variability compared to the remotely sensed burned area. Model II has a much lower performance not only in the total agreement reached (R-value), but also in the representation of the spatial pattern (Appendix, Fig. A1).

3.1 Inter-annual variability

To evaluate the performance of the models over the years we also investigated the inter-annual variability, in this case using the estimated parameters to predict not only the evaluation dataset but the full dataset. The predicted burned area ratios were further used to calculate the simulated inter-annual variation using the standard deviation for each grid cell between years. The spatial distribution of the inter-annual variability of burned area as detected by MODIS and predicted by model I is shown in Fig. 5 (model II Fig. A1, Appendix). Though areas experiencing a high inter-annual variability are correctly depicted, the total amount of the inter-annual variability is underestimated by model I.

3.2 Intra-annual variability

The two Hovmöller diagrams Fig. 6 and 7 display the intra-annual distribution of the wildfires and the Nesterov index. The highest fire activity in the Northern Hemisphere is detected between October and February and in the southern part the majority of wildfires occur between May and October. In both hemispheres the burn seasons shift to later periods from north to south. The fire season in the northern part is shorter and more pronounced than in the Southern Hemisphere where the burning especially

BGD
7, 4385–4424, 2010

south of 10° S occurs over a longer time-span at a low level.

The Nesterov index, a cumulative index of the dryness is limited, according to our definition, to a maximum of 2×10^5, which was reached only in the Saharan desert. Figure 7 indicates that the timing of the dry season depends strongly on latitude. For the Northern Hemisphere coinciding with the majority of fires, the dry season starts in September and lasts until May, while in the latitudinal band where wildfires occur in the Southern Hemisphere it lasts from May until September. Visual comparison of the two diagrams (Fig. 6 and Fig. 7) shows that the majority of fires occur at the beginning of the dry season.

In order to find a quantitative relation between the burned area and the dryness, we binned the values of the logarithms of the Nesterov index (Ni) and added all the burned area fractions, for each bin. After scaling the values to total area of one we fitted a lognormal distribution (Fig. 8; Eq. 6). The result can be interpreted as a probability density for the fire activity. The maximum is found at a Nesterov index of ca. 10^4, more precisely the parameter μ of the fitted lognormal distribution equals to 3.95 and the parameter σ to 0.495. The relative fraction burned ba_r can hence be estimated for each day using Eq. 6.

$$ba_r = \frac{1}{\sqrt{2\pi\sigma^2}} \exp \frac{-(\log_{10} Ni - \mu)^2}{2\sigma} \tag{6}$$

To check the resulting relationship between the relative burned area and the Nesterov index we used the test area between 20° E and 30° E (Fig. 1) and correlated the calculated sums of burned area fractions as estimated from Eq. 6 with the observed ones. The resulting R-value is 0.89 ($p < 0.001$). The relationship in Eq. 6 can be used to add an intra-annual time dependence to our model. This is shown for an example grid cell in Fig. 9. Panel (a) displays the Nesterov index over the year 2007. Using Eq. 6 we then distribute the relative fraction burned over the year. Finally we scale the prediction of the fraction burned given by our model (Eq. 5) so that the total sum of the relative fractions (Eq. 6) equals the burned area estimated from Eq. 5 and obtain

BGD
7, 4385–4424, 2010

panel (c). A comparison with the observed burned area distribution (Fig. 9b) shows a good agreement between the timing of the observed and predicted burned area, with a smoother seasonal course in the statistical model than observed by the satellite. The predicted burned area (Fig. 9c) shows two peaks in November while MODIS senses no fire activities around that time. This is caused by the fact that our prediction of the timing of the fire activities depends solely on the Nesterov index. If a short dry period within the wet season causes the Nesterov index to reach values indicating a fire potential, it predicts a fire activity regardless of the time of the year. However, since these periods are relatively short, the total error in terms of the intra-annual fire distribution is rather small.

3.3 Model application – simulated burned area

Applying the two burned area models with simulated climate and population data results in the total burned areas displayed in Fig. 10. At continental scale, all climate variables considered show only small changes over time (Fig. 2). However, the displayed total values include not only the savannah regions (since their extend might change over time) but also the tropical rain forest and the large deserts, hence local differences in the savannah regions might not be reflected in this figure. While the total precipitation is similar in the climate simulations based on the two SRES storylines, the Nesterov index as well as the total population reaches higher values in the A2 scenario.

Figure 10 displays the simulated burned area for the time period form 1980 to 2060 which decreases over time in all simulations. The variability of model I (Fig. 10a and b) is smaller than the variability of model II (Fig. 10c and d) which takes only the climate variables into account. The decrease of model I lies at ca. $0.3\times10^{12}\,km^2$ (ca. 20–25% of maximum value) in both hemispheres, though the total values are lower in the Southern Hemisphere (Fig. 10a and b). Model II estimates lower burned areas, a lower decrease as well as a larger inter-annual variability. The simulation based on the SRES A2 storyline results in higher burned areas though the differences are not significant, since the standard deviations of the total burned areas of both scenarios overlap in the majority of cases.

BGD
7, 4385–4424, 2010

4 Discussion

The correct simulation and prediction of continental or global wildfire pattern is, despite of being interesting in itself, a crucial part in the predictive modelling of vegetation distribution, structure, and the exchanges of greenhouse gases and pyrogenic substances. The presented statistical analysis has been especially designed for its suitability in this respect, noting that the necessary choice of a sub-set of applicable variables might lead to a lower performance compared to other approaches that are not restricted in the choice of the explanatory data (e.g. Archibald et al., 2008).

However, the selected variables: precipitation, Nesterov index (reflecting potential fuel dryness and being related to precipitation), tree and herb cover, and population density are key determinants of fire patterns (Archibald et al., 2008) and are available for historic and projected time periods or commonly simulated within DVMs. This aspect as well as the simplicity of the model (being a generalized linear model) allows a straightforward implementation in DVMs or GCMs. Model I represents the spatial distribution of area burnt well, but the inter-annual variability and maximum burn fraction is underestimated. One likely reason for the underestimation of temporal and spatial variability is the broad geographic scale at which the analysis is performed. Both individual fires as well as precipitation vary substantially well below the spatial resolution of this analysis which is performed on a one-degree spatial grid. We are also aware that additional variables influence the annual burned area, like landscape fragmentation (density of roads), differences in the developmental stage of the agricultural systems and the fire suppression policy (e.g. Archibald et al., 2008) or land use, since the application of fires is strongly linked to human activity. The latter is probably the variable with the highest explanatory value. However, the simulation of land use pattern is not common within current DVMs and while a projection of land use changes is available for the 21th century for Europe (Reginster and Rounsevell, 2006), nothing comparable is available for the African continent to the knowledge of the authors.

BGD
7, 4385–4424, 2010

Additionally, the variable herb cover which had the highest explanatory value is only available as a static dataset for the year 2001. This is problematic for the development of the statistic model since fire can potentially have strong impacts on tree and herb cover over time and therefore change their distribution (Arneth et al., 2010a). Given the uncertainty in the burned area data (see Methods section) and high level of aggregation due to the required one degree scale, we consider our agreement between the final model and the data reasonable.

The analysis showed clearly that the vegetation and productivity related variables i.e. tree and herb cover as well as precipitation over the last 4 seasons and over the preceding wet season are ranked above variables relating to the dryness of the fuel i.e. precipitation over the dry season and Nesterov index (Table 1). This indicates that in the majority of cases the fuel load is by far more important for the area burnt than the dryness, since the dry season in most parts of African savannas are sufficiently long to generate fire prone conditions. The difference in the predictive power of the two models also shows that the estimation of burned area is strongly enhanced by the use of vegetation derived variables. These variables should ideally have an at least an annual resolution in order to further increase the predictive power of the model. Our results show however, that even the incorporation of a single year of vegetation related data like tree and herb cover increases the predictive power of the burned area model strongly.

An earlier fire model for the application in DVMs or GCMs was developed by Pechony et al. (2009), using similar driving variables but additionally accounting for lightning as a driver. Though lightning is assumed to be the only natural ignition source potentially resulting in a considerable amount of wildfires, we decided not to include this variable because natural ignitions are likely of minor importance in Africa, at least under the present day fire regime (Saarnak, 2001). Additionally, the spatial resolution of the remotely sensed lightning data e.g. 2.5 degree, Christian et al., 1996) and the data quality of the available daily resolution products is not sufficient to estimate natural ignitions. A previous attempt to use these data showed that it is problematic to separate

BGD
7, 4385–4424, 2010

between lighting strikes occurring before the rain event and strikes which occur during a rain event, imposing a much lower risk of fire ignition (Arneth et al., 2010a). Ignition caused by lighting is thereby prone to be overestimated using the currently available global datasets. Still, for model applications that seek to study changes in fire regimes into the past or into the future a separate treatment of lightning is desirable because the paleo-record of fire puts forward strong arguments for a mostly climate-driven fire regime (Marlon et al., 2008), and since climate change is expected to change patterns of thunderstorms and lightning (Price and Asfur, 2006). Even though fires are in most cases ignited by people for a variety of purposes (land management, hunting, agriculture practices; Saarnak, 2001) our study shows that climate variables are still more important factors in explaining fire occurrence than population density. As a matter of fact, no prescribed ignition would succeed without favourable environmental conditions and even though our study shows that low fire activity is also associated with very low population density, at the spatial scale used in the analysis we can hardly represent the uneven population distribution occurring within a grid cell. Therefore, at this spatial level, we do not expect a clear correlation between population and fires, but this correlation would be probably significantly increased on a finer spatial scale. From the investigated variables, population density is likely to have the highest spatial variability. Our results are confirmed by the findings of Archibald et al. (2008) who also ranked the importance of population density below all climate and vegetation related drivers of burned area (though still at the fifth rank out of 11 investigated drivers). Their study, which was conducted at a comparable resolution found no evidence that ignition frequency either limited or promoted the burnt area. High population densities however are linked to low fire frequencies due to fire prevention or low fuel load. Due to the scale of this analysis where each grid cell varies in its extend from 1.2×10^4 km^2 at the equator to 1.0×10^4 km^2 at the most northern part of Africa, even though a high population density might be assigned to a certain cell, parts of the cell might still be less densely populated and hence subject to wildfires.

BGD
7, 4385–4424, 2010

Our assessment of model performance was based on the R-value and the BIC. Relying solely on R-values might be problematic in cases of nonlinear relationships, and can potentially lead to over-fitting by ignoring the number of parameters used for the analysis. By contrast, the BIC applies a weight to the number of variables to select the best model (Schwarz, 1978). All factors considered in our regression model represent certain aspects of the conditions that determine the overall burned area, and the BIC statistics did not provide a strong argument to discard any of these although their relative importance will vary. In addition to causal correlation, a considerable amount of spatial correlation is present in the explanatory as well as in the predicted variables. We separated the available datasets into groups and tested the model performance only on data not used to estimate the fire model parameter. But since our model focuses on the continental wildfire patterns for large-scale applications rather than analyzing causal relationships per se, a complete analysis of the influence of the spatial autocorrelation on the variables is beyond the scope of this work. Our listing of the driving variables thus also does not consider a ranking or effects including variables in different order which has been done in some analyses.

In our analysis we used a "fire year" instead of the Julian year and shifted the seasons between northern and southern Africa to pool all available data in a meaningful way. However when performing a parameterization for a global model (e.g. Pechony and Shindell, 2009) we consider a distinction between different regions necessary, like it was done by (Giglio et al., 2006) for the estimation of the ratio between detected active fires ("hot spots") and burned area. Considerable variation exists between regions in their fire regime and/or the use of fire as a land management tool, and this has to be reflected in the parameterization of the fire model. It is to be expected, for instance, that a parameterisation for mean precipitation of the last four seasons, which has shown a strong influence on the African fires would not work in boreal forests. For Africa, precipitation is the main driver of productivity and hence available litter to burn, while in cooler environments, accumulated temperature becomes an additional important factor (Crevoisier et al., 2007).

BGD
7, 4385–4424, 2010

To the knowledge of the authors, this study is the first to propose a procedure to distribute fire events over the course of the year. The correct timing of the simulated fires is important since the effects of fires on vegetation strongly depend on fire intensity and hence on the climatic conditions determining the fuel dryness. We related timing of fires to the fuel dryness represented by the Nesterov index. The found is uni-modal relationship with a peak at a medium value of the Nesterov index indicates that the time of ignition is chosen to be at the beginning of the dry season which confirms to Saarnak (2001). We expect a natural fire regime to result in a higher amount of burned area at high Nesterov index values caused by lightning strikes just before the wet season (dry lightning) which, though rare in numbers, could potentially burn large areas that would have a high fuel accumulation in the absence of a human driven fire regime. Over the course of the year, the Nesterov index as displayed in Fig. 7 decreases less abrupt than shown in Fig. 9a, and distributing the burned area temporally from such smooth transitions could potentially lead to an incorrectly simulated second fire season at the end of the dry season. However, the smooth transition in Fig. 7 is caused by the latitudinal and inter-annual averaging. At a single cell, the Nesterov–index drops from the maximum level to zero at the first day with 3 mm or more precipitation (Fig. 9a). Within a dynamic vegetation model, the daily fraction of burned area can hence directly be calculated from Nesterov index using Eq. 5 and 6.

The application of the parameterised burned area models resulted in a considerable decrease of burned area regardless of the scenario and applied model. This is of major concern for the inhabitants of the area since a high fire frequency in Africa, where it was applied as a land management tool since millennia, is an indictor for an area suitable for a variety of human activities to produce food. The vast majority (ca. 90%) of the Africa's population depends on rain-fed crop production and pastoralism within the savannah biome to meet its basic food supplies (Patt and Winkler, 2007). The simulated burned areas for the year 1997 to 2008 of model I are comparable to the values estimated by Giglio et al. (2010) who list values between $1.1{\cdot}10^{12}$m^{2}and $1.5{\times}10^{12}$ m^2 with a mean of $1.31{\cdot}10^{12}$m^2 for the northern and a similar range, but a slightly smaller mean of

BGD
7, 4385–4424, 2010

1.25×10^{12} m^2 for the Southern Hemisphere of Africa. This encourages the use of the simulated climate data in connection with the parameterized model I since the climate data used here is (though for an overlapping time period) an independent simulation of the climate variables from the GCM which also generated the future projection of the climate. Since both models resulted in R-values indicating a considerable uncertainty in the estimation of the burned area, we consider the total figures of burned area as rough estimates, especially since the analysis has shown that climate alone is a rather weak predictor of burned area. However, the decreasing trend of burned area over the next decades is, regardless of the total value, a consisted feature. A decreasing trend is at least for the Northern Hemisphere also to be seen in the remotely sensed burned areas of Giglio et al. (2010). The underestimation of the burned area by model II is probably related to the low total performance of the model. However, even in model II the decreasing trend is visible. The model containing the full variable set resulted in a lower variability since we assumed the tree, as well as the herb cover not to change with time. This in turn stabilized the estimated burned area compared to the model including only climate variables.

The fact that the total precipitation (2 years mean, dry and wet season precipitation) show no obvious trend over time (current time as well as the future), but the burned area decrease indicates, that the GCM assumes the spatial distribution to change and the climatic range suitable for wildfires is shrinking accordingly. This is in agreement with the IPCC 4th Assessment report which states that during recent decades, eastern Africa has been experiencing an intensifying dipole rainfall pattern with increasing rainfall over the northern sector and decreased rainfall over the southern sector (Schreck and Semazzi, 2004; in Boko et al., 2007). The small differences in the simulated burned area between the different scenarios show that they do not differ strongly in the most important drivers of fire and the differences in the increase in population has only limited influence on the total burned area since the population is expected to grow mainly in highly populated areas which cover only a small proportion of the African continent.

BGD
7, 4385–4424, 2010

5 Conclusions

Understanding fire driving factors is fundamentally important for developing process-based simulation models of fire occurrence under future climate and environmental change scenarios. This study offers a tool to estimate burned area for a variety of purposes. It provides both, the estimation of the total burned area as well as the intra-annual distribution of the fire activity over the year. The application of the models to climate change projections shows the potential of the derived model and the strong decrease in burned area which is related to favourable conditions for food production demonstrates the impact that the expected climatic changes will have for Africa.

Appendix A

Parameter and performance of model II (Burned area model with reduced variable set)

The general form of model II is similar to the form of model I conforming to Eq. A1. Instead of seven, the reduced set has only 5 parameter, as listed in Table A1. The predicted ratios of area burned are given in Fig. A1.

Similar to model I, we used the natural logarithm instead of the actual value for the variables dry season precipitation and population density.

$$ba = \frac{1}{1 + e^{-\left(a + \sum_{i=1}^{5} l_i v_i + s_i v_i^2\right)}} \quad \text{(A1)}$$

For further information refer to the explanation given for Eq. 5.

BGD
7, 4385–4424, 2010

Acknowledgements. This study was funded by the European Commission by the 6th FP project CarboAfrica. The comments of Sally Archibald on this manuscript are acknowledged.

References

Archibald, S., Roy, D. P., van Wilgen, B. W., and Scholes, R. J.: What limits fire? An examination of drivers of burnt area in Southern Africa, Glob Change Biol, 15, 613–630, doi:10.1111/j.1365-2486.2008.01754.x, 2009.

Arneth, A., Lehsten, V., Spessa, A., and Thonicke, K.: Climate-fire interactions and savanna ecosystems: a dynamic vegetation modelling study for the African continent, in: Ecosystem Function in Savannas: Measurement and Modeling at Landscape to Global Scales, edited by: Hill, M. J. and Hanan, N. P., CRC Press, 2010a.

Arneth, A., Sitch, S., Bondeau, A., Butterbach-Bahl, K., Foster, P., Gedney, N., de Noblet-Ducoudré, N., Prentice, I. C., Sanderson, M., Thonicke, K., Wania, R., and Zaehle, S.: From biota to chemistry and climate: towards a comprehensive description of trace gas exchange between the biosphere and atmosphere, Biogeosciences Discuss., 6, 7717–7788, doi:10.5194/bgd-6-7717-2009, 2009.

Bengtsson, M., Shen, Y. J., and Oki, T.: A SRES-based gridded global populatiou dataset for 1990–2100, Population and Environment, 28, 113–131, doi:10.1007/s11111-007-0035-8, 2006.

Bird, M. I. and Cali, J. A.: A million-year record of fire in sub-Saharan Africa, Nature, 394, 767–769, 1998.

Boko, M., Niang, I., Nyong, A., Vogel, C., Githeko, A., Medany, M., Osman-Elasha, B., Tabo, R., and Yanda, P.: Africa, in: Climate Change 2007: Impacts, Adaptation and Vulnerability. Contribution of Working Group II to the Fourth Assessment Report of the Intergovernmental Panel on Climate Change, edited by: Parry, M. L., Canziani, O. F., Palutikof, J. P., Linden, P. J. v. d., and Hanson, C. E., Cambridge University Press, Cambridge UK, 433–467, 2007.

Christian, H. J., Driscoll, K. T., Goodman, S. J., Blakeslee, R. J., Mach, D. A., and Buechler, D. E.: The Optical Transient Detector (OTD), 10th International Conference on Atmospheric Electricity, Osaka, Japan, 1996.

Crevoisier, C., Shevliakova, E., Gloor, M., Wirth, C., and Pacala, S.: Drivers of fire in the boreal forests: Data constrained design of a prognostic model of burned area for use in dynamic

BGD

7, 4385–4424, 2010

global vegetation models,, J. Geophys. Res., 112, D24112, doi:10.1029/2006JD008372, 2007.
Foken, T.: Angewandte Meteorologie, Springer Verlag, Berlin, 2003.
Giglio, L., van der Werf, G. R., Randerson, J. T., Collatz, G. J., and Kasibhatla, P.: Global estimation of burned area using MODIS active fire observations, Atmos. Chem. Phys., 6, 957–974, doi:10.5194/acp-6-957-2006, 2006.
Giglio, L., Randerson, J. T., van der Werf, G. R., Kasibhatla, P. S., Collatz, G. J., Morton, D. C., and DeFries, R. S.: Assessing variability and long-term trends in burned area by merging multiple satellite fire products, Biogeosciences, 7, 1171–1186, doi:10.5194/bg-7-1171-2010, 2010.
Hansen, M. C., DeFries, R. S., Townshend, J. R. G., Carroll, M., Dimiceli, C., and Sohlberg, R. A.: Global Percent Tree Cover at a Spatial Resolution of 500 Meters: First Results of the MODIS Vegetation Continuous Fields Algorithm, Earth Interact, 7, 2003.
Harris, S., Tapper, N., Packham, D., Orlove, B., and Nicholls, N.: The relationship between the monsoonal summer rain and dry-season fire activity of northern Australia, Int. J. Wildland Fire, 17, 674–684, doi:10.1071/wf06160, 2008.
Healy, E.: Population density in, FAO-UN; available at http://www.fao.org/geonetwork/, 2008.
Hough, J. L.: Why burn the bush? Social approaches to bush-fire management in West African National parks, Biol. Conserv., 65, 23–28, 1993.
Kummerow, C., Barnes, W., Kozu, T., Shiue, J., and Simpson, J.: The Tropical Rainfall Measuring Mission (TRMM) sensor package, J. Atmos. Ocean.-Tech., 15, 809–817, 1998.
Lehsten, V., Tansey, K., Balzter, H., Thonicke, K., Spessa, A., Weber, U., Smith, B., and Arneth, A.: Estimating carbon emissions from African wildfires, Biogeosciences, 6, 349–360, doi:10.5194/bg-6-349-2009, 2009.
Lehsten, V., Arneth, A., Thonicke, K., and Spessa, A.: Tree-Grass Coexistence in Savannahs: Testing Two Mechanisms, in review, 2010.
Marlon, J. R., Bartlein, P. J., Carcaillet, C., Gavin, D. G., Harrison, S. P., Higuera, P. E., Joos, F., Power, M. J., and Prentice, I. C.: Climate and human influences on global biomass burning over the past two millennia, Nat. Geosci., 1, 697–702, 2008.
Mbow, C., Goita, K., and Benie, G. B.: Spectral indices and fire behavior simulation for fire risk assessment in savanna ecosystems, Remote Sens. Environ., 91, 1–13, doi:10.1016/j.rse.200310.019, 2004.
Mbow, C., Nielsen, T. T., and Rasmussen K.: Savanna Fires in East-Central Senegal: Dis-

BGD
7, 4385–4424, 2010

tribution Patterns, Resource Management and Perceptions, Hum. Ecol. Spec. Issue, 28, 561–583, 2000.
Nesterov, V. G.: Gorimost' lesa i metody eio opredelenia., Goslesbumaga, 1–75, 1949.
Patt, A. G. and Winkler, J.: Applying climate information in Africa: an assessment of current knowledge, Boston University, 2007.
Pechony, O. and Shindell, D. T.: Fire parameterization on a global scale, J. Geophys. Res., 114, D16115, doi:10.1029/2009JD011927, 2009.
Potter, C. S., Randerson, J. T., Field, C. B., Matson, P. A., Vitousek, P. M., Mooney, H. A., and Klooster, S. A.: Terrestrial ecosystem production – A process model based on global satellite and surface data, Global Biogeochem. Cy., 7, 811–841, 1993.
Price, C. and Asfur, M.: Inferred long term trends in lightning activity over Africa, Earth Planets Space, 58, 1197–1201, 2006.
Reginster, I. and Rounsevell, M.: Scenarios of future urban land use in Europe, Environ. Plann. B., 33, 619–636, 2006.
Roeckner: IPCC MPI-ECHAM5_T63L31 MPI-OM_GR1.5L40 20C3M_all run no.1: atmosphere 6 HOUR values, in: MPImet/MaD Germany, World Data Center for Climate., 2005.
Roy, D. P., Boschetti, L., Justice, C. O., and Ju, J.: The Collection 5 MODIS Burned Area Product – Global Evaluation by Comparison with the MODIS Active Fire Product, Remote Sens. Environ., 112, 3690–3707, 2008.
Roy, P. D., Ju, J., Mbow, C., Frost, P., and Loveland, T.: Accessing free Landsat data via the Internet: Africa's challenge, Remote Sens. Lett., 1, 111–117, 2010.
Saarnak, C. F.: A shift from natural to human-driven fire regime: implications for trace-gas emissions, Holocene, 11, 373–375, 2001.
Schreck, C. J. and Semazzi, F. H. M.: Variability of the recent climate of eastern Africa, Int. J. Climatol., 24, 681–701, 2004.
Schwarz, G.: Estimating the Dimension of a Model, Annals of Statistic, 6, 461–464, 1978.
Smith, B., Prentice, I. C., and Sykes, M. T.: Representation of vegetation dynamics in the modelling of terrestrial ecosystems: comparing two contrasting approaches within European climate space, Glob. Ecol. Biogeogr., 10, 621–637, 2001.
Spessa, A., McBeth, B., and Prentice, C.: Relationships among fire frequency, rainfall and vegetation patterns in the wet-dry tropics of northern Australia: an analysis based on NOAA-AVHRR data, Glob. Ecol. Biogeogr., 14, 439–454, 2005.
Thonicke, K., Spessa, A., Prentice, I. C., Harrison, S. P., Dong, L., and Carmona-Moreno, C.:

BGD
7, 4385–4424, 2010

The influence of vegetation, fire spread and fire behaviour on biomass burning and trace gas emissions: results from a process-based model, Biogeosciences Discuss., 7, 697–743, doi:10.5194/bgd-7-697-2010, 2010.

van der Werf, G. R., Randerson, J. T., Giglio, L., Collatz, G. J., Kasibhatla, P. S., and Arellano Jr., A. F.: Interannual variability in global biomass burning emissions from 1997 to 2004, Atmos. Chem. Phys., 6, 3423–3441, doi:10.5194/acp-6-3423-2006, 2006.

Van Wilgen, B. W., Govender, N., Biggs, H. C., Ntsala, D., and Funda, X. N.: Response of Savanna fire regimes to changing fire-management policies in a large African National Park, Conserv. Biol., 18, 1533–1540, 2004.

Venevsky, S., Thonicke, K., Sitch, S., and Cramer, W.: Simulating fire regimes in human-dominated ecosystems: Iberian Peninsula case study, Glob. Change Biol., 8, 984–998, 2002.

Williams, C. A., Hanan, N. P., Neff, J. C., Scholes, R. J., Berry, J. A., Denning, A. S., and Baker, D. F.: Africa and the global carbon cycle, Carbon Balance and Management, 2:3, 2007.

BGD
7, 4385–4424, 2010

Table 1. Parameterisation of model I. Correlation coefficient (R-value) of all models with variables used as single predictors; constant linear and squared coefficients of the single variable models and model I. The correlation coefficients are derived by correlating the fractions of burned area estimated for the test dataset covering the longitudinal band from 20° E till 30° E with the observed fractions of burned area. The constant term for the final model I (a) is −10.06.The abbreviations a, v, l and s are used in Eq. 5.

Model variables (v)	Corr. coeff. single var. model	Constant term single var. model (a)	Linear coeff. in single var. model (l)	Squared coeff. in single var. model (s)	Linear coeff. in final model (l)	Squared coeff. in final model (s)
Tree-cover [ratio]	0.53	−4.20	$2.10\ 10^{-1}$	$-4.01\ 10^{-3}$	$1.69\ 10^{-1}$	$-1.49\ 10^{-3}$
Mean Precipitation last 4 seas. [mm]	0.49	−6.55	$1.00\ 10^{-2}$	$-3.92\ 10^{-6}$	$3.22\ 10^{-3}$	$-1.29\ 10^{-6}$
Herb-cover [ratio]	0.43	−8.13	$1.63\ 10^{-1}$	$-8.20\ 10^{-4}$	8.7810^{-3}	$7.41\ 10^{-4}$
Precipitation Rain-season [mm]	0.46	−5.76	$9.51\ 10^{-3}$	$-4.08\ 10^{-6}$	-3.6910^{-4}	$2.66\ 10^{-7}$
Nesterov maximum [see above]	0.39	−2.54	$3.68\ 10^{-5}$	$-3.71\ 10^{-10}$	$1.95\ 10^{-5}$	-6.6810^{-11}
log(Population density [per/km^2])	0.27	−2.94	2.09	−1.63	-6.7810^{-1}	$-8.03\ 10^{-2}$
log(Precipitation Dry-season [mm])	0.26	−5.72	3.62	$-6.89\ 10^{-1}$	-4.4310^{-1}	$2.66\ 10^{-1}$

BGD
7, 4385–4424, 2010

Table A1. Parameterisation of model II. Correlation coefficient (R-value) of all single variable models and constant linear and squared coefficients model II. The correlation coefficients are derived by correlating the fractions of burned area estimated for the test dataset covering the longitudinal band from 20° E till 30° E with the observed fractions of burned area. The constant term for the final model II (a) is −7.91. The abbreviations a, v, l and s are used in Eq. A1.

Model variables (v)	Corr. coeff. single var. model	Linear coeff. in final model (l)	Squared coeff. in final model (s)
Mean Precipitation last 4 seas. [mm]	0.49	$8.66\ 10^{-3}$	-3.6210^{-6}
Precipitation Rain-season [mm]	0.46	9.6810^{-4}	-3.0710^{-7}
Nesterov maximum [see above]	0.39	$3.80\ 10^{-5}$	-1.9310^{-10}
log(Population density [per/km^2])	0.27	-5.7210^{-2}	$-2.29\ 10^{-1}$
log(Precipitation Dry-season [mm])	0.26	3.9110^{-1}	-4.9510^{-2}

BGD
7, 4385–4424, 2010

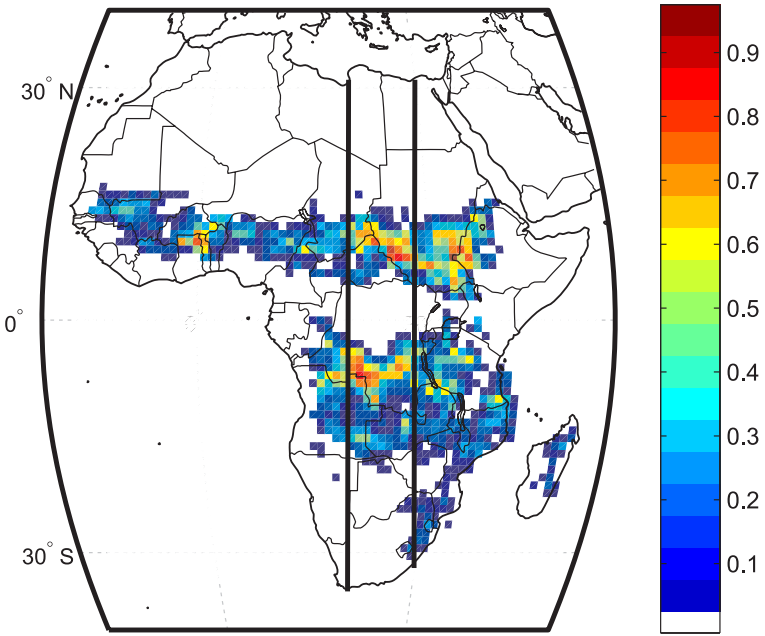

Fig. 1. Mean annual fraction of area burned, averaged over all investigated years from 2000–2007. Data resulting from grid cells outside the two plotted meridians is used as training data, to estimated the model parameter, except for the data for the year 2007. The data from grid cells between the two meridians is only used to estimate the R-values.

BGD
7, 4385–4424, 2010

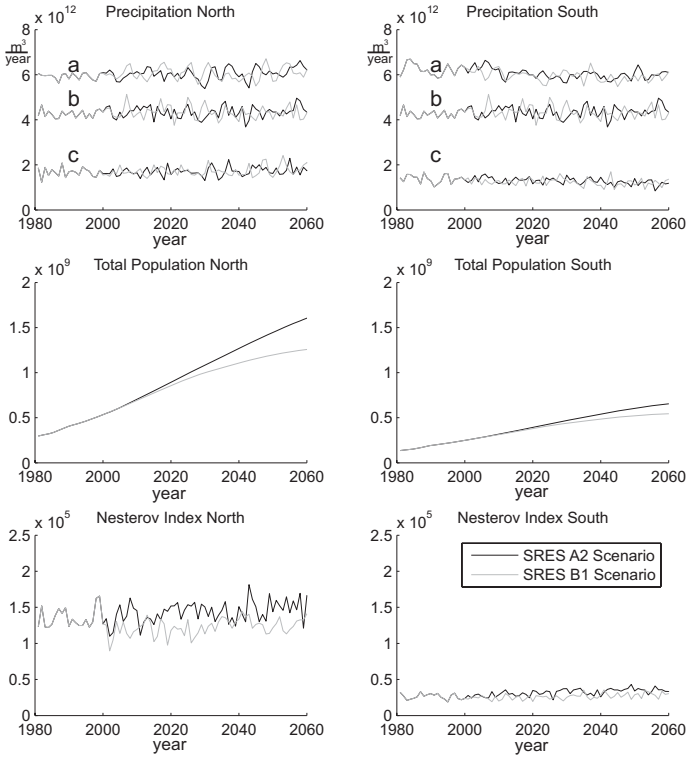

Fig. 2. Simulated climate and population variables used to project the burned area untill the year 2060 for the two SRES storylines A2 and B1. The time period from 1980 untill 2000 is calculated from the control simulation of the 20th century and is therefore similar for both scenario runs. For details of the used data sets see the Methods section. Upper panels: total precipitation: a-lines : mean annual precipitation over the last 4 seasons (covering 2 years); b-lines: total precipitation wet season; c-lines total precipitation dry season; middle panels: total population, lower panels Nesterov index, mean of maximum values of each year.

BGD
7, 4385–4424, 2010

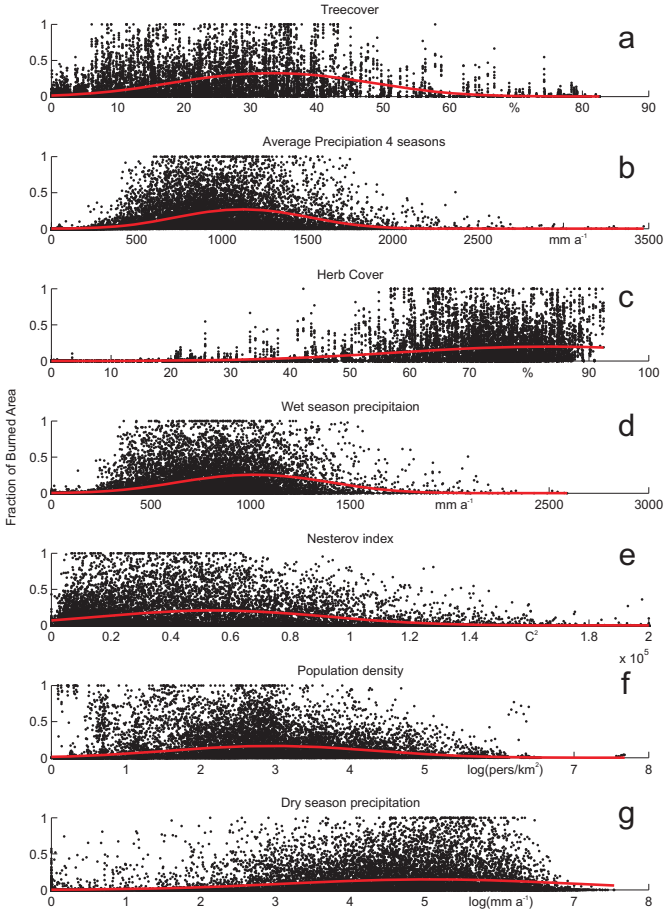

Fig. 3. Response of burned area to the variables tree and herb cover, precipitation (average over the last four seasons, last wet, last dry season) and population density. The correlation coefficients as well as the model parameter for each variable are listed in Table 1.

BGD
7, 4385–4424, 2010

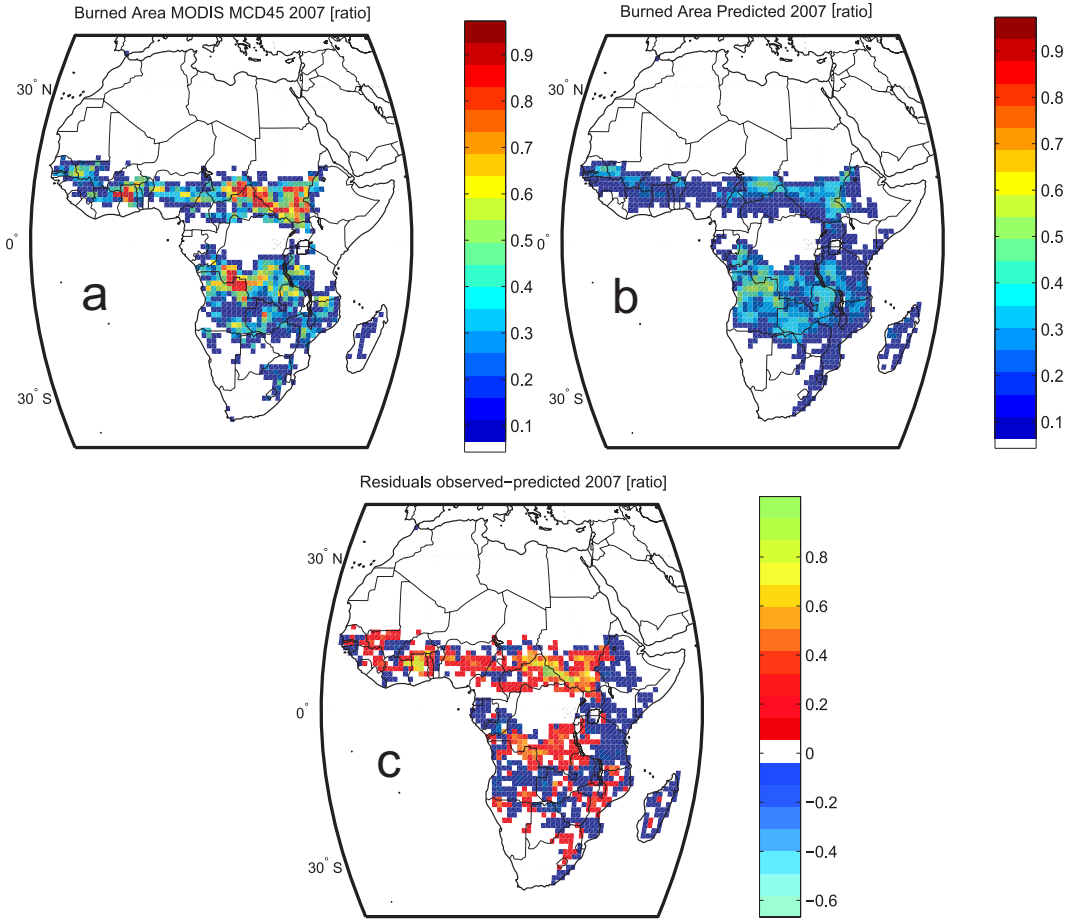

Fig. 4. Standard deviation of fraction of burned area from 2000 to 2008, **(a)** directly derived from MODIS burned area product MCD45; **(b)** predicted from the fire model, using all available years.

BGD
7, 4385–4424, 2010

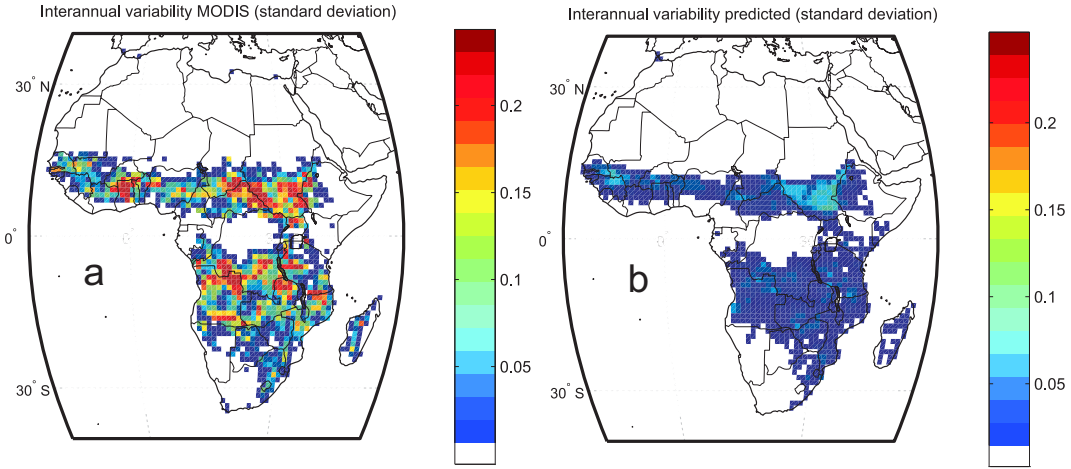

Fig. 5. Standard deviation of fraction of burned area from 2000 to 2008, **(a)** directly derived from MODIS burned area product MCD45; **(b)** predicted from the fire model, using all available years.

BGD
7, 4385–4424, 2010

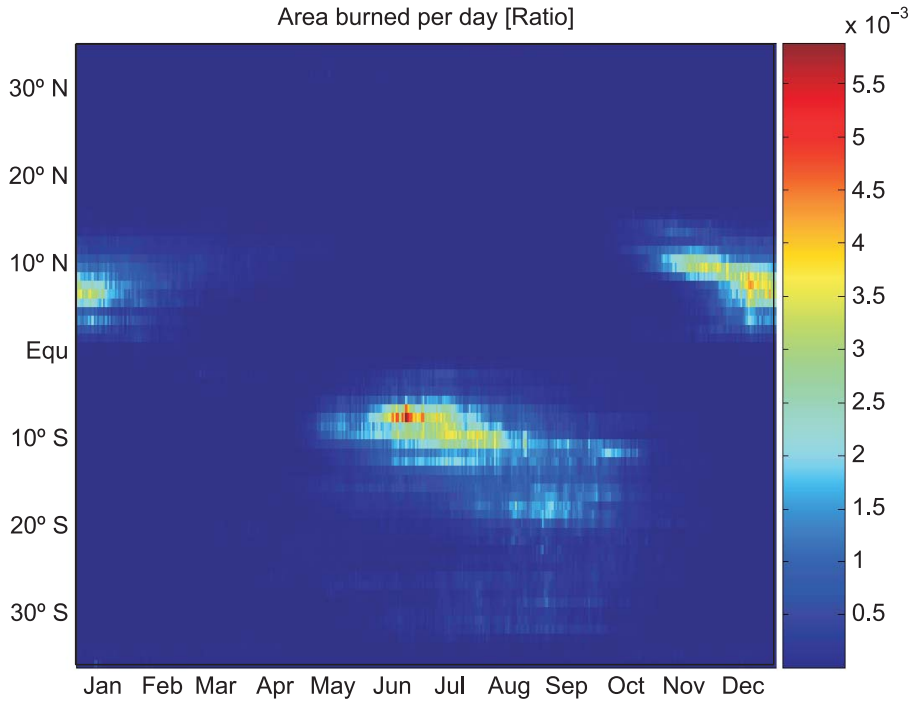

Fig. 6. Hovmöller diagram of daily ratio of burned area per day, averaged over the period from 2000–2008.

BGD
7, 4385–4424, 2010

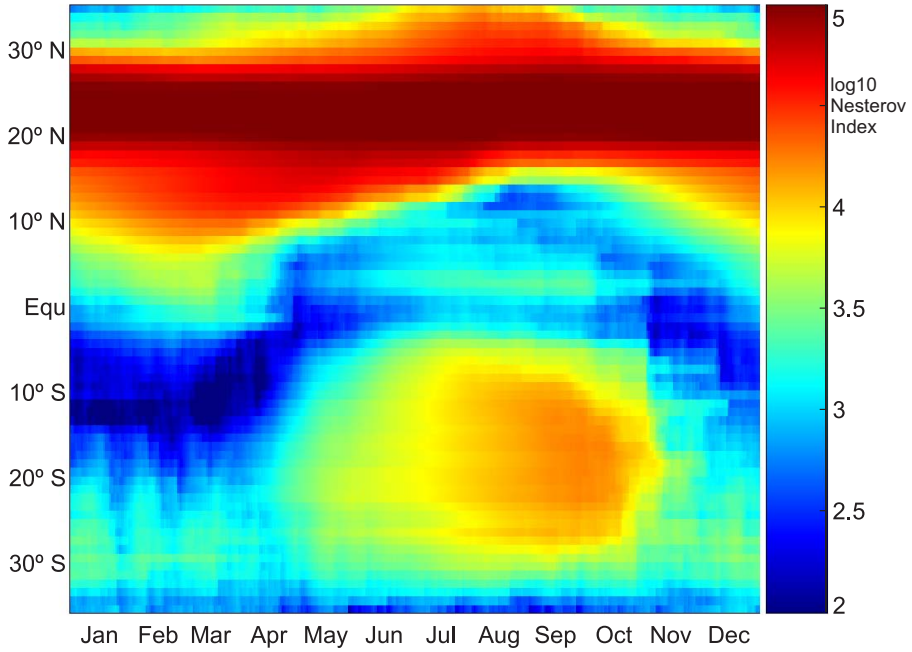

Fig. 7. Hovmöller diagram of daily latitudinal averages of the Nesterov index, averaged over the period from 2000–2008. The red areas between 20° N and 30° N are for the Saharan desert where the Nesterov index was never reset to zero by a sufficient rain even (more than 3 mm per day) during the investigation period.

BGD
7, 4385–4424, 2010

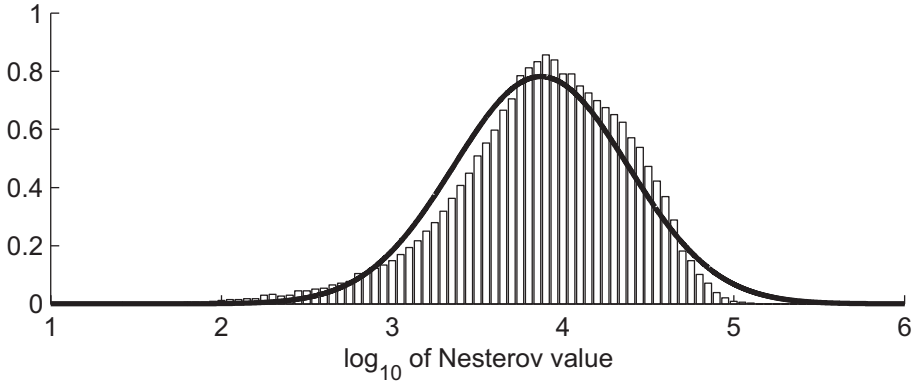

Fig. 8. Sum of burned area fractions versus the $\log_{10}$ of the Nesterov indices rescaled to area 1. This curve was generated using the same training data as used in the remaining analysis (i.e. all locations outside the area from 20° E to 30° E).

BGD
7, 4385–4424, 2010

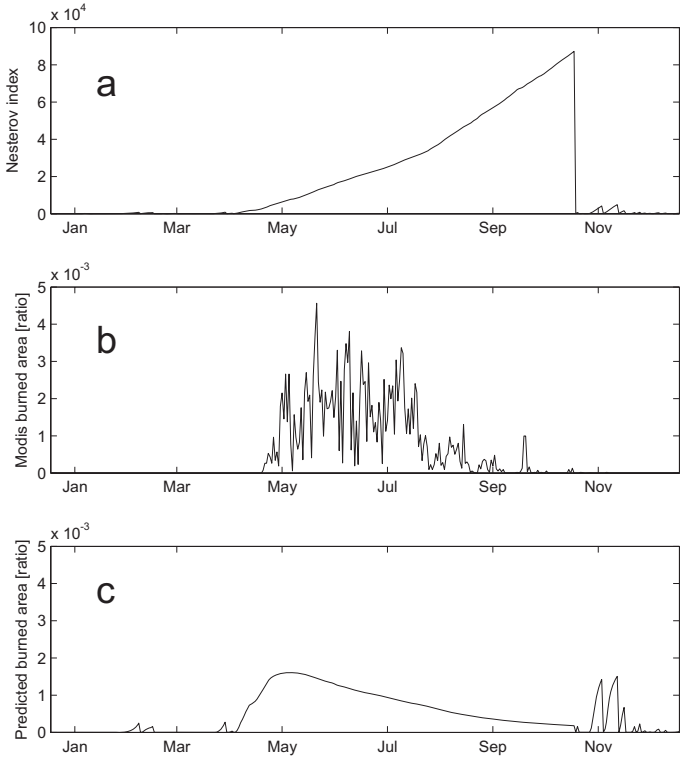

Fig. 9. Intra-annual wildfire activity. Temporal distribution of Nesterov index **(a)**, the observed burned area **(b)** and the predicted temporal distribution of ratio burned **(c)** for an example gridcell for the year 2007 (−12° S and 27° E).

BGD
7, 4385–4424, 2010

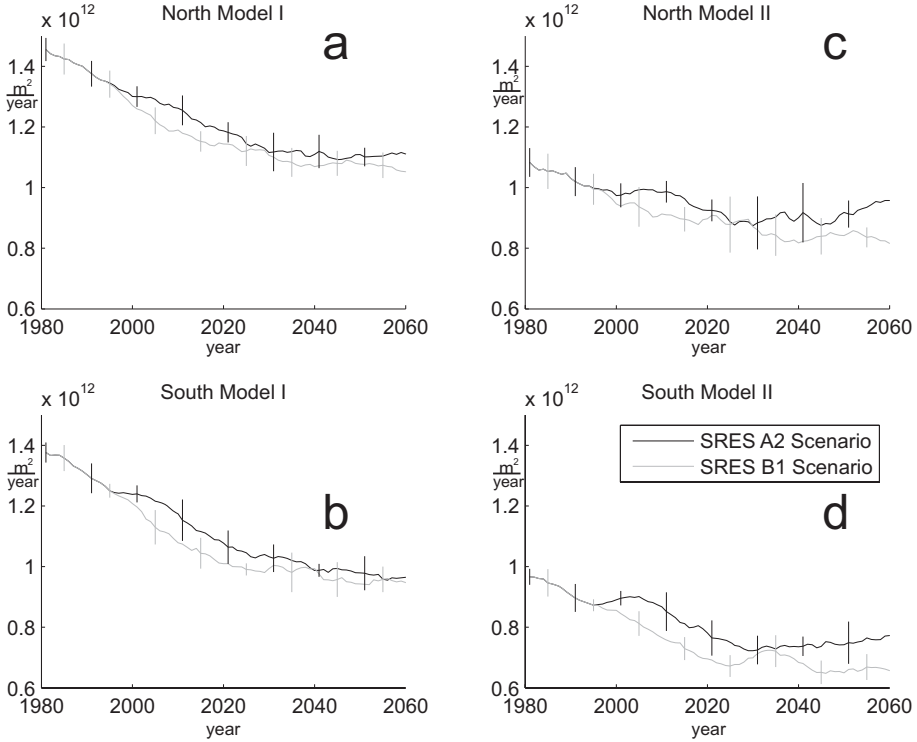

Fig. 10. Projected burned area of the northern (panel **a** and **c**) and Southern (panel **b** and **d**) Hemisphere of Africa using model I (panel a and b) and model II (panel c and d) for the two SRES storylines A2 and B1 from 1980–2060. The time period from 1980–2000 is derived from the control simulation of the 20th century. Lines are moving averages of 10 years and bars show the standard deviation within the 10 years.

BGD
7, 4385–4424, 2010

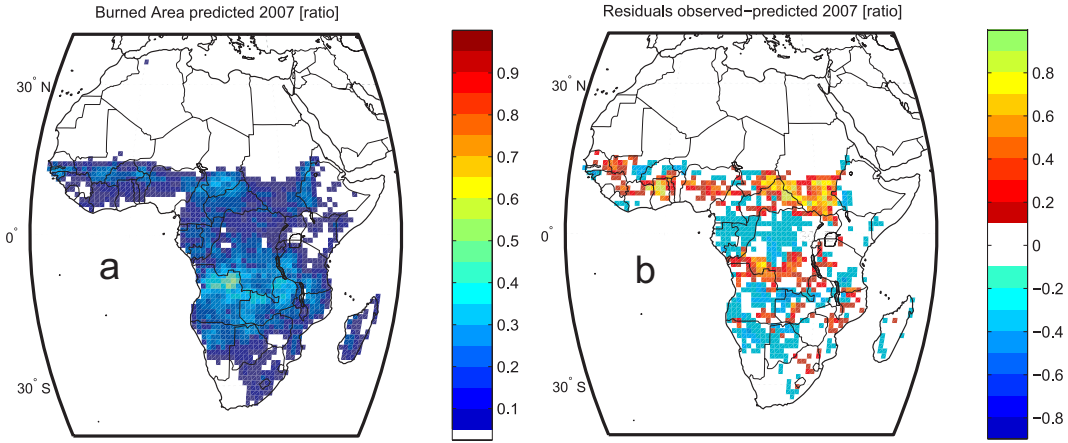

Fig. A1. Fraction of area burned in the fire year 2007. Panel **(a)** predicted from the parameterised fire model II. Panel **(b)** residuals observed (remotely sensed from MODIS MCD45; see Fig. 4 panel a) – predicted from model II. Data for the year 2007 is not used for the estimation of the model parameter (Table A1).

BGD
7, 4385–4424, 2010